Composite Structures 288 (2022) 115443

Contents lists available at ScienceDirect

Composite Structures

journal homepage: www.elsevier.com/locate/compstruct

Shear performance of basalt fiber-reinforced concrete beams reinforced with BFRP bars

Ahmed El Refai [a], Wael Alnahhal [b,*], Abathar Al-Hamrani [b], Sarah Hamed [a]

[a] Department of Civil and Water Engineering, Laval University, Quebec, Canada
[b] Department of Civil and Architectural Engineering, Qatar University, Doha, Qatar

ARTICLE INFO

Keywords:
Shear
Basalt fibers
BFRP bars
Slender beams
Short beams
Basalt fiber-reinforced concrete

ABSTRACT

This paper reports on the experimental and analytical investigation of the shear performance of concrete beams cast with basalt fiber-reinforced concrete (BFRC) and longitudinally reinforced with basalt fiber-reinforced polymer (BFRP) bars. Fourteen hybrid (BFRC-BFRP) beams with no stirrups were tested to failure under a four-point loading setup. The investigated parameters included the volume fraction, V_f, of the added fibers (0.75 and 1.5%), the reinforcement ratio of the BFRP bars,ρ, (0.31, 0.48, 0.69, 1.05, and 1.52%), and the shear span-to-depth ratios, a/d, of the beams (3.3 and 2.5 for slender and short beams, respectively). The tests results showed that adding 0.75% of basalt macrofibres (BMF) improved the shear capacity of the slender and short beams by 46 and 43 %, respectively, compared to 81 and 82% when 1.5% of BMF were added. The impact of adding the BMF on the shear strength of the beams diminished as the longitudinal reinforcement ratios increased. The existing models overestimated the shear strength of the tested beams with an average predicted-to-experimental ratio ranging between 1.15 ± 0.03 and 2.48 ± 0.29. A shear model that accounts for the type of the longitudinal reinforcement and the added fibers was proposed to predict the shear strength of the BFRC-BFRP beams. A good agreement between the predicted and experimental shear strength was evident with a predicted-to-experimental ratio that ranged between 0.98 ± 0.11 and 0.88 ± 0.02 for the slender and short beams, respectively.

1. Introduction and background

Reinforced concrete (RC) beams develop their shear strength through a well-established mechanism that involves friction forces, compressive forces, and aggregate interlocking over the tension-shear cracks. Beside those governing parameters, the dowel action of the reinforcing bars, which develops as the shear crack grows and cuts across the bars, is a major contributor to the shear strength, particularly in beams with no stirrups provided. Typically, as the longitudinal reinforcement ratio,ρ, increases, the dowel action's contribution to the shear capacity of the beam increases.

RC beams with fiber-reinforced polymer (FRP) bars usually exhibit wider and extended cracks than their conventional steel-reinforced counterparts due to the lower modulus of the FRP bars. Therefore, FRP-reinforced beams acquire lower shear capacities than their steel-reinforced counterparts [1–5]. Demands to assess the contribution of FRP bars to the shear strength have been raised after their recognition as main reinforcement in most codes and design guidelines [6–8]. Issa et al. [9] investigated the shear strength of concrete beams reinforced with basalt FRP (BFRP) bars. The authors reported a 32% gain in the shear strength when the reinforcement ratio of the BFRP bars, ρ, was increased from 0.8% to 1% and it was further enhanced by 54.3% at a higher ρ of 2%. El Refai and Abed [10] observed that increasing the reinforcement ratio of the BFRP bars from 0.31% to 1.5% in the tested beams resulted in 76% increase in their shear capacity. In addition, beams with a shear span-to-depth (a/d) ratio of 2.5 had shear capacities that were 14 to 45% higher than those with (a/d) ratio of 3.3.

Shear is brittle in nature and therefore, with the weak dowel action of FRP reinforcement in mind, enhancing the concrete characteristics may become an efficient approach to increase its shear resistance. Several studies have reported that using high strength concrete mixes would offset the poor transverse resistance of the FRP bars [11,12]. Said et al. [13] observed that using high concrete compressive strength ($f_c^{'}$) of 45 MPa and 70 MPa has improved the shear capacity of concrete beams reinforced with glass FRP (GFRP) bars by 49 and 104%, respectively, over an identical beam with low ($f_c^{'}$) of 20 MPa. Other studies suggested

* Corresponding author.
E-mail addresses: ahmed.elrefai@gci.ulaval.ca (A. El Refai), wael.alnahhal@qu.edu.qa (W. Alnahhal), aa1205725@qu.edu.qa (A. Al-Hamrani), Sarah.Hamed.1@ulaval.ca (S. Hamed).

https://doi.org/10.1016/j.compstruct.2022.115443
Received 24 November 2021; Received in revised form 15 February 2022; Accepted 2 March 2022
Available online 6 March 2022

Table 1
Test matrix of the experimental program.

Beam	No. of BFRP bars	ρ%	ρ/ρ_b	V_f %
Group A ($a/d = 3.3$)				
A-R1-0*	2 – 8 M	0.31	1.09	0
A-R1-0.75				0.75
A-R1-1.5				1.5
A-R2-0*	2 – 10 M	0.48	1.69	0
A-R2-0.75				0.75
A-R2-1.5				1.5
A-R3-0*	2 – 12 M	0.69	2.43	0
A-R3-0.75				0.75
A-R3-1.5				1.5
A-R4-0*	4 – 10 M	1.05	3.69	0
A-R4-0.75				0.75
A-R4-1.5				1.5
A-R5-0*	4 – 12 M	1.52	5.35	0
A-R5-0.75				0.75
A-R5-1.5				1.5
Group B ($a/d = 2.5$)				
B-R1-0*	2 – 8 M	0.31	1.09	0
B-R1-0.75				0.75
B-R1-1.5				1.5
B-R3-0*	2 – 12 M	0.69	2.43	0
B-R3-0.75				0.75
B-R3-1.5				1.5

* Beams reported from El Refai and Abed [10].

that using fiber-reinforced concrete (FRC) mixes was an attractive alternative to increase the shear capacity of FRP-reinforced beams [14–17]. As reported by Li et al. [18], the random dispersion of the discrete fibers in FRC mixes created an even resistance to stresses in all directions. The fibers played a major role in postponing the formation of cracks in concrete and, as the applied loads increased, they bridged the formed cracks and prevented the splitting of concrete. This bridging mechanism increased the contribution of concrete to the shear resistance as reported by Ding et al. [21]. Moreover, Minelli and Plizzari [22] stated that adding fibers has modified the mode of failure of the tested specimens into ductile flexural failure rather than a brittle shear failure. Furthermore, the addfibers has largely improved the shear capacities of both normal and high-strength concrete [23].

Recently, new fibers made of BFRP have emerged as substitutes to

Table 2
Constituents of the concrete mix.

Type	Quantity (kg/m^3)
Cement	440
Fly ash	50
Water	149.6
Coarse aggregates	1158
Fine aggregates	752
Super plasticizer	8.8

Table 3
Compression test results.

V_f %	Sample	$f`_c$, MPa	Average$f`_c$, MPa	SD	COV %
0.75	1	59.88	57.49	1.56	2.71
	2	58.14			
	3	56.99			
	4	55.97			
	5	56.46			
1.5	1	63.38	63.47	5.60	8.80
	2	60.76			
	3	69.85			
	4	67.65			
	5	55.71			

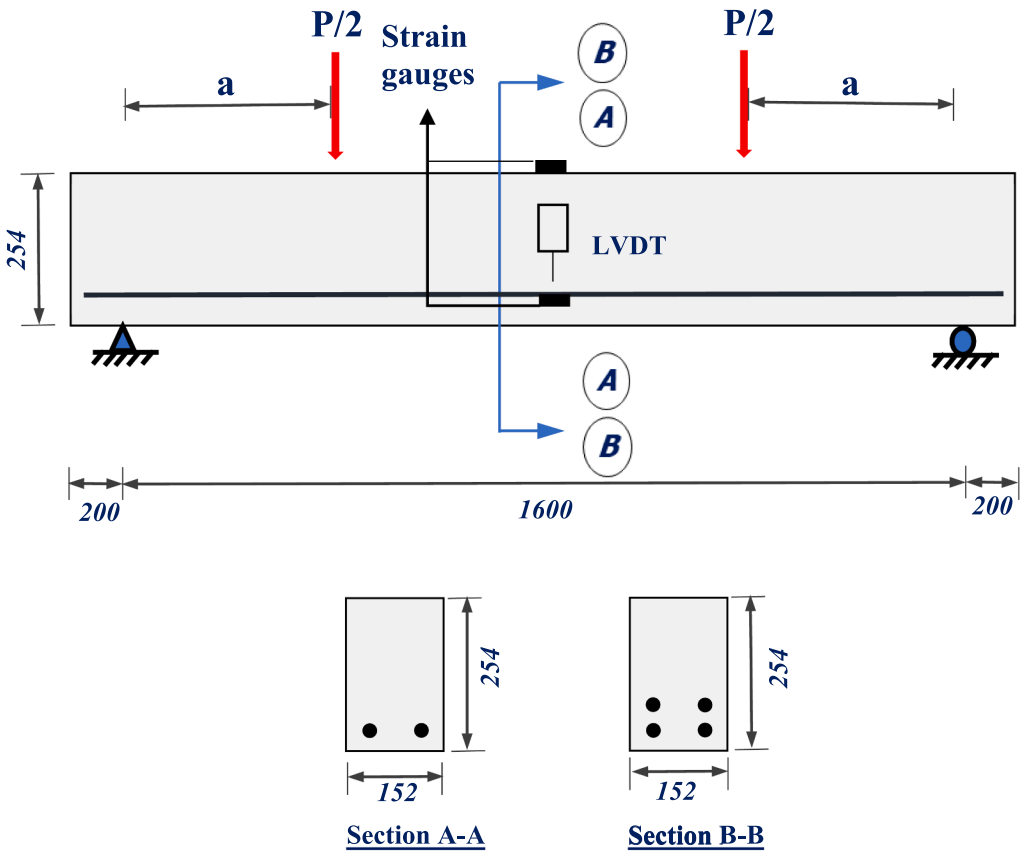

Fig. 1. Dimensions and reinforcement details of the beam specimen (all dimensions are in *mm*).

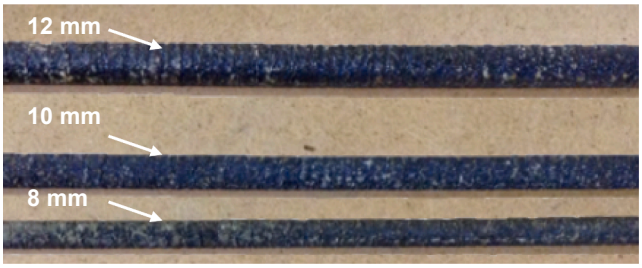

Fig. 2. The BFRP bars used in reinforcing the tested beams.

Fig. 3. The basalt macro-fibers (BMF) used in this study.

traditional synthetic and steel fibers. These novel basalt macro-fibers (BMF) are recognized by their relatively high modulus of elasticity in comparison with other synthetic fibers, their high tensile strength, their anti-corrosive nature, and their efficiency in impeding the crack propagation in concrete [24,25]. The BMF are also recognized by their non-toxic and inert nature [26]. In comparison to conventional plain concrete, the basalt fiber-reinforced concrete (BFRC) demonstrated enhanced tensile properties, improved flexural toughness, and showed higher modulus of rupture and higher $f_c^{'}$ as reported in [27,28]. In the present study, experimental tests were carried out on hybrid BFRC-BFRP concrete beams that were cast with BFRC mix (having different volume fractions of BMF) and reinforced with BFRP longitudinal bars (having different reinforcement ratios) to study their shear behavior. The experimental tests were followed by an analytical study aiming to assess the feasibility of the available shear formulations, which were initially developed for structures cast with conventional FRC mixes and reinforced with conventional steel bars, to estimate the shear strength of the hybrid BFRC-BFRP beams. From the analytical investigation, a new model was proposed and validated against the test results obtained in the current study.

2. Research program

The experimental program consisted of fourteen RC beams as shown in Table 1. Two groups of beams (A and B) were tested according to their a/d ratios. All beams were reinforced with reinforcement ratios, ρ, greater than the balanced reinforcement ratio, ρ_b, as recommended by the CAN/CSA-S806-12 [8] code and the ACI-440.1R-15 [6] guidelines. Beams of group A were reinforced with five different ratios, ρ, namely; 1.09 ρ_b, 1.69 ρ_b, 2.43 ρ_b, 3.69 ρ_b, and 5.35 ρ_b with a span-to-depth ratio, a/d, of 3.3. Beams of group B were reinforced with two ratios, ρ, of 1.09 ρ_b and 2.43 ρ_b with a/d ratio of 2.5. The ρ_b was calculated as per the ACI-440.1R-15 guidelines [6]. Two volume fractions, V_f, of BMF, namely; 0.75 and 1.5% were added to the concrete mix. In addition, seven BFRP-reinforced beams previously reported in El Refai and Abed [10] and cast with plain concrete ($V_f = 0\%$) were used as benchmarks for the tested beams. Those beams had the same dimensions and ρ values as their counterparts in groups A and B. It is important to note that the beams of El Refai and Abed [10] had the same type and dosage of their constituent materials and were cured for the same duration as those of the current study to ensure that all beams had similar mechanical properties of concrete.

2.1. Beam specimen

Fig. 1 illustrates the reinforcement details and beam dimensions. The beams were 2 m long with a rectangular cross section of 254 × 152 mm and a clear cover of 30 mm. BFRP bars placed at the bottom (tension) side of the beams were used as the main longitudinal reinforcement. All beams were designed to encounter a shear failure and thus, no transverse reinforcement was provided. The beams are labeled in X-Y-Z format, where 'X' indicates the beam group (A or B), 'Y' indicates the

Fig. 4. (a) Four-point-load configuration (b) LVDT placed at midspan.

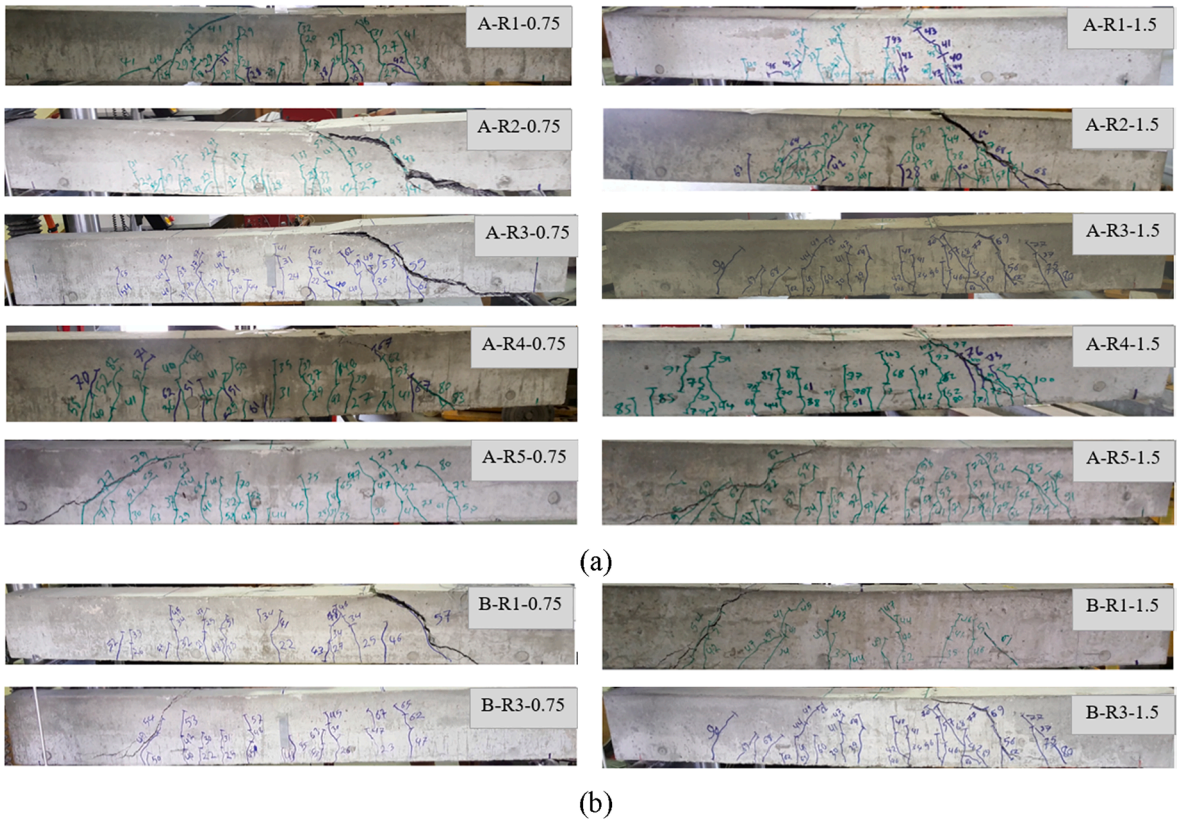

Fig. 5. Crack patterns and failure of beams of (a) group A and (b) group B.

Fig. 6. Bridging effect during testing of beam A-R2-0.75.

longitudinal reinforcement ratio that varies between R1 and R5, representing 1.09, 1.69, 2.43, 3.69, and 5.35 ρ_b, respectively, and 'Z' indicates the volume fraction of BMF provided in the concrete mix, V_f, which varies between 0 (plain concrete), 0.75, and 1.5%.

2.2. Material properties

The constituents of the concrete mix used to cast the beams are shown in Table 2. Five standard cylinders of size 150 × 300 mm were also cast and cured simultaneously with the beams. Compression tests were performed according to ASTM C469 [29] provisions. While the $f_c^{'}$ of the plain concrete mix achieved 49 MPa as recorded by El Refai and Abed [10], the BFRC mix with $V_f = 0.75\%$ achieved an average $f_c^{'}$ of 57.5 MPa, representing a gain in the compressive strength of 17% compared to a 30% gain in strength for the mix with V_f of 1.5%, as listed in Table 3.

BFRP bars with diameters 8, 10, and 12 mm were used. The actual diameters measured by immersion were 8.2, 10.2, and 12.2 mm, respectively. The actual diameters were used in the design of the BFRC-BFRP beams and succeeding analysis. Fig. 2 shows the BFRP bars used in reinforcing the tested beams. The BFRP bars had a tensile strength, modulus of elasticity, and ultimate strain of 1168 MPa, 48 GPa, and 0.023, respectively, as reported by the manufacturer.

The BMF shown in Fig. 3 had a helical shape and a rough surface to enhance their bond to concrete. The BMF had a diameter,D_f, of 0.66 mm with length, L_f, of 43 mm. These dimensions corresponded to an aspect ratio,$\frac{L_f}{D_f}$, of 65.15. As stated in the manufacturer's datasheet, the BMF had a tensile strength of 1100 MPa, modulus of elasticity of 45 GPa, and a density of 1900 kg/m^3.

2.3. Instrumentation and testing setup

As can be depicted from Fig. 1, the tested beams were instrumented with 60 mm long strain gauges fixed on the extreme compression side of the beams' midspan. In addition, 5 mm long strain gauges were attached to the middle of the BFRP bars to record strain changes at various loading phases. Each beam was simply supported and loaded in a four-point configuration as shown in Fig. 4. A data acquisition was used to record data from the LVDTs and strain gauges.

3. Test results

3.1. Crack pattern and failure mode

The crack patterns for beams of groups A and B are illustrated in Fig. 5 (a) and (b), respectively. Initially, flexural cracks were formed at midspan and propagated progressively upwards towards the extreme

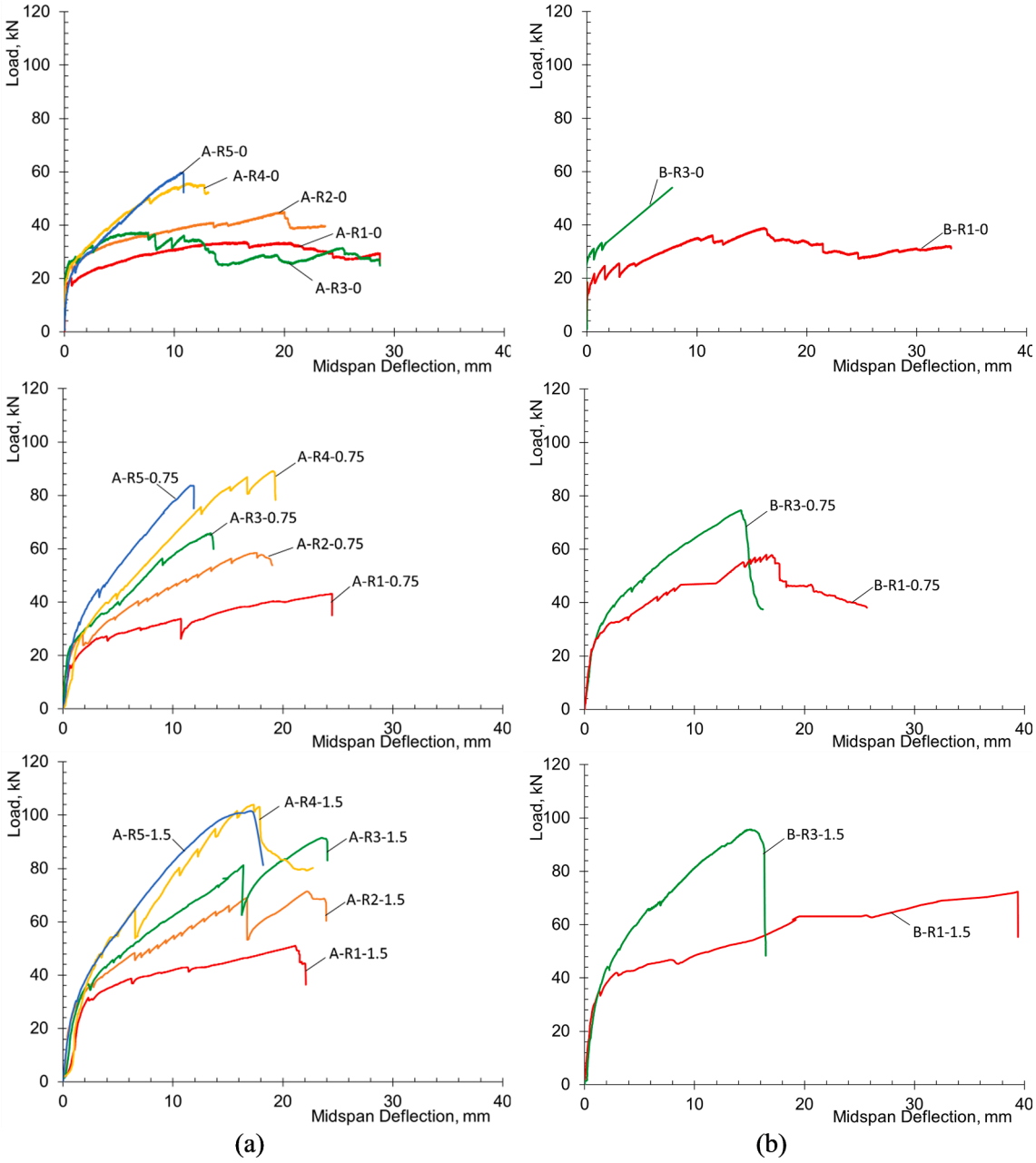

Fig. 7. Load-deflection response for beams of (a) group A and (b) group B.

compression zone. As the applied load increased, the flexural cracks increased in width and height while new cracks were formed. When the applied loads were further increased, diagonal cracks were formed along the shear span and extended towards the loading points until failure occurred. All beams failed in shear as a result of one main diagonal crack as shown in Fig. 5.

Beams cast with BFRC encountered more flexural cracks than their control counterparts. It was observed that the BMF not only postponed the formation of the cracks, but also bridged the formed cracks and prevented concrete splitting in the post-cracking stage as can be depicted from Fig. 6 for beam A-R2-0.75, where the fibers kept the two failed sections intact until pullout of the fibers occurred. These observations were similar to those reported in Attia et al. [30] on BFRC-cast slabs tested in flexure, in which the number of flexural cracks developed in the maximum moment zone increased as the volume fraction of the BMF increased. Sahoo et al. [31] also reported similar observations when 1% of polypropylene and steel fibers were added to conventional RC beams with no shear stirrups provided.

Despite some discrepancies, it was noticed that beams with high V_f of fibers or high ρ experienced flatter shear cracks, as shown in Fig. 5. The BMF played the role of additional reinforcement that contributed to the development of the shear resistance of the beams hence, lessening the angle at which the shear cracks were generated. However, the scattered orientation of the BMF in the concrete mix caused the discrepancies observed in the inclination of the shear cracks in all of the tested beams. The BFRC beams of group B exhibited more inclined shear cracks than those of group A. The inclination of the cracks in beams of group B ranged between 45 and 65° compared to 28 and 55° in those of group A. This expected finding was attributed to the variation in the a/d ratios of both groups of beams.

3.2. Load-deflection and load–strain responses

Fig. 7 shows the load–deflection response of the tested beams. All

Table 4
Summary of the experimental results.

Beam	P_{cr}, kN	P_{ult}, kN	V_{ult}, kN	V_{BMF}, kN**	δ_{max}, mm	Measured strains $\times 10^{-6}$		Angle of shear failure, degrees
						BFRP bar	Concrete	
	Group A (a/d = 3.3)							
A-R1-0*	13.5	33.8	16.9	–	24	12,400	−2400	55
A-R1-0.75	16.3	43.1	21.5	4.7	24.4	20,764	−1540	48
A-R1-1.5	22.4	50.9	25.4	8.6	29.0	13,406	−904	53
A-R2-0*	15	46.2	23.1	–	23.1	1040	−1100	55
A-R2-0.75	24.5	58.5	29.2	6.2	19	11,812	−1387	34
A-R2-1.5	25.2	71.3	35.6	11.4	24.5	12,642	−1232	40
A-R3-0*	13	37.2	18.6	–	28.7	10,600	−1800	44
A-R3-0.75	19.3	65.7	32.8	14.3	13.7	8747	−1484	31
A-R3-1.5	29.7	91.5	45.7	21.9	24	10,644	−2176	55
A-R4-0*	20.6	55.7	27.8	–	13	5600	−1800	25
A-R4-0.75	23.6	89.1	44.5	15.7	19.3	9137	−1816	30
A-R4-1.5	26.2	103.9	51.9	23	23.8	10,390	−1792	36
A-R5-0*	27.5	59.8	29.9	–	10.8	5400	−1900	32
A-R5-0.75	27.6	83.6	41.8	11.6	14.3	6465	−1461	28
A-R5-1.5	29.4	100.8	50.4	20.5	18.7	7778	−2117	28
	Group B (a/d = 2.5)							
B-R1-0*	14.5	39	19.5	–	26.3	10,700	−1500	45
B-R1-0.75	21.7	57.9	28.9	9.4	25.6	7628	−1552	45
B-R1-1.5	28.9	72.4	36.2	7.3	42.1	13,147	−2586	47
B-R3-0*	20.8	54	27	–	7.1	6300	−1500	65
B-R3-0.75	20.5	74.5	37.2	10.25	16.2	8497	−1470	45
B-R3-1.5	34.3	95.7	47.8	20.8	16.5	7793	−987	45

* Data adopted from El Refai and Abed[10] P_{cr} = cracking load; P_{ult} = ultimate load; V_{ult} = shear capacity; δ_{max} = maximum midspan deflection.
** Contribution of BMF taken as V_{ult} (current study) - V_{ult} (El Refai and Abed [10] study).

beams exhibited linear relationships in their deflection responses until the initiation of the first crack. At this stage, the midspan deflections in the beams were negligible, in particular for beams of group B with a/d ratio of 2.5.

At the onset of the post-cracking stage, all beams encountered a drop in their stiffness due to the widening of the existing cracks and the formation of new cracks. The post-cracking stiffness of the beams varied according to their ρ and the provided amounts of BMF. Beams with high ρ encountered higher post-cracking stiffness than those with lowρ, yet less than their pre-cracking stiffness. This was obvious from the post-cracking stiffness curves of beams A-R1-0.75 and A-R2-0.75, as examples. Similar findings were encountered in beams of group B as can be depicted from the plots of Fig. 7b.

The results summarized in Table 4 show that the impact of the reinforcement ratio,ρ, on the post-cracking stiffness of beams of group A was more pronounced than those of group B. Beams of group A, with high a/d ratio, tended to change their mode of failure towards a more flexural mode while those of group B, with low a/d ratio, were governed by the arch action in which stresses are resisted by compressive struts and tensile ties rather than the ρ value.

Similarly, beams cast with high V_f of fibers displayed lower deflections and higher post-cracking stiffness than those cast with low V_f of fibers. As previously mentioned, the added fibers played the role of additional reinforcement that limited the opening of the existing cracks and thus, impeded the loss of the beams' stiffness. Such role diminished as ρ increased, which suggested that the post-cracking response was essentially governed by the reinforcement ratio as clearly shown in Fig. 7a for BFRC-beams with ρ of R4 and R5. The addition of BMF in those beams resulted in a gain in their post-cracking stiffness compared to their control beams. However, the gain in stiffness was much less than those observed in beams with low ρ (beams with R1, R2, and R3).

The strains measured in both the concrete and BFRP bars during testing are shown in Figs. 8 and 9 for beams of groups A and B, respectively. All beams demonstrated linear relationships in their strain response prior to the initiation of the first flexural crack. At this stage, the recorded strains in the BFRP bars were almost nil. Once cracking occurred, all beams encountered a significant increase in their measured strains, which was accompanied by a reduction in their stiffness as previously described. The increase in strains was less pronounced in beams with higher reinforcement ratios and higher V_f of BMF. This observation illustrates the effectiveness of the BMF in reducing the tensile stresses in the longitudinal bars due to the bridging effect. However, for beams having different V_f of BMF, the effect of fibers on reducing the post-cracking strains in beams having high reinforcement ratios (of R4 and R5) was less pronounced than in beams having low reinforcement ratios (ρ of R1, R2, and R3). It is important to note the significant impact that the reinforcement ratio had on the recorded strains in the post-cracking stage. Beams with high reinforcement ratios showed a notable reduction in their recorded strains when compared to those with low reinforcement ratios at the same level of loading. For instance, the strain recorded in the BFRP bars of beam A-R2-0.75 at load 57 kN was 12,000 με while that recorded in beam A-R5-0.75 at the same load was only 3600 με. On the other hand, the a/d ratio provided had a significant effect on the strain response of the beams. Beams of group B recorded significantly less strains than their counterparts of group A. For instance, the strain recorded in the BFRP bars of beam A-R1-1.5 (with a/d = 3.3) was 13,000 με at load 50 kN whereas that recorded in beam B-R1-1.5 (a/d = 2.5) at the same load was 7000 με. This finding was attributed to the increased moment arm in sections of beams with higher a/d ratio, which induced higher stresses in the longitudinal bars.

3.3. Shear capacity

Fig. 10 (a) and (b) presents the intercorrelation between the obtained shear capacity, the reinforcement ratios,ρ, and the volume fraction, V_f, of BMF used for beams of groups A and B, respectively. The lowest curve in Fig. 10 represents the control beams cast with plain concrete while the upper two curves represent those cast with BFRC mixes at V_f = 0.75 and 1.5%.

The obtained trend in Fig. 10 (a) and (b) revealed that the increase of ρ resulted in a significant increase in the shear capacity of the tested beams irrespective of their a/d ratios or the V_f of the added fibers. Beams

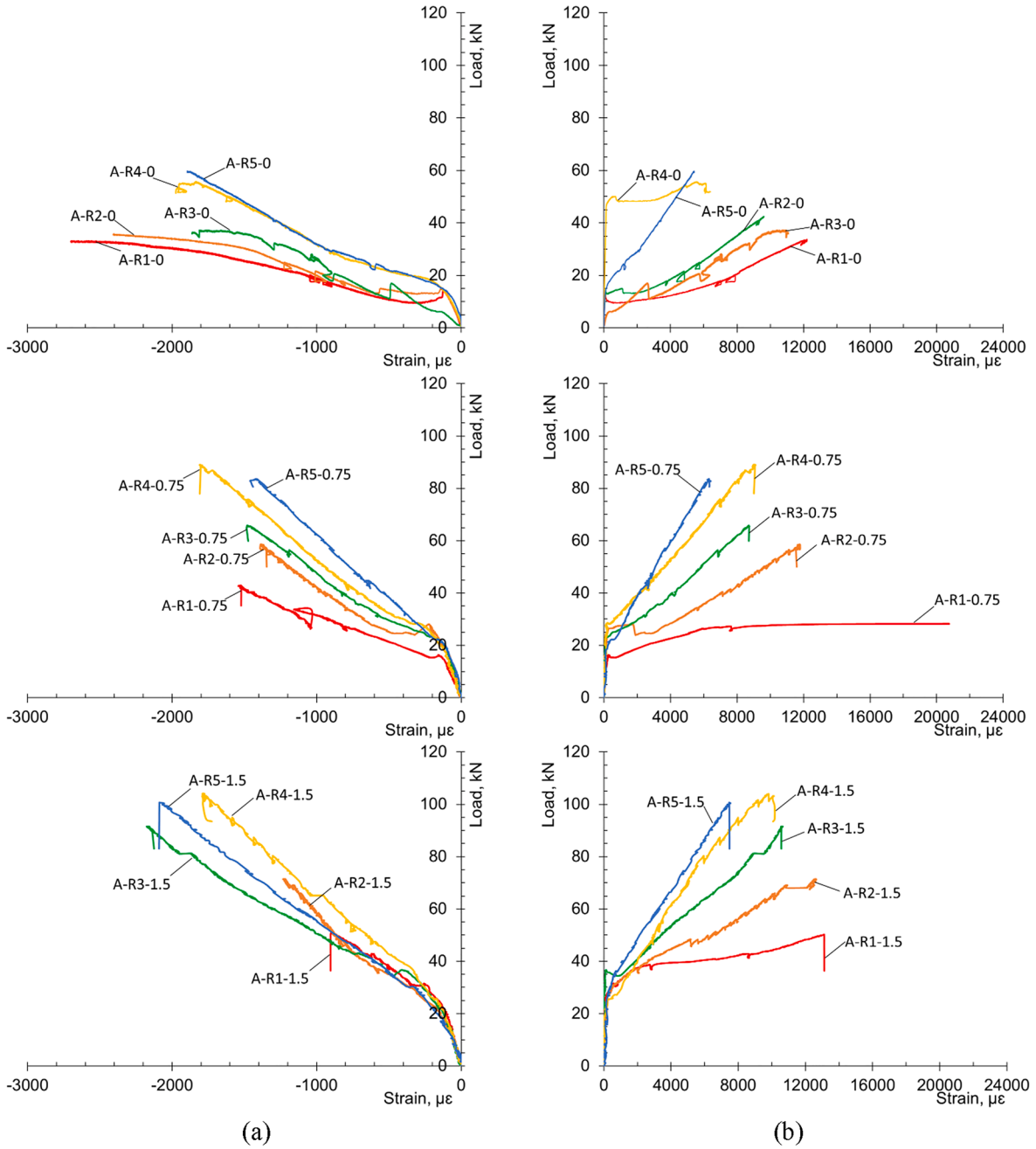

Fig. 8. Load-strain response of beams of group A: (a) strains in concrete and (b) strains in the BFRP bars.

of group A with ρ values ranging between R1 ($\rho = 1.09\ \rho_b$) and R4 ($\rho = 3.69\ \rho_b$) showed a nearly linear increase in their shear capacity. Beyond R4 ($\rho = 3.69\ \rho_b$), an almost flat pattern was observed demonstrating the diminishing effect of the dowel action of the BFRP bars on the shear capacity of the beams. This finding was obvious from the results obtained for beams A-R4-0.75 and A-R5-0.75 (and beams A-R4-1.5 and A-R5-1.5) that showed almost similar shear capacity despite the difference in their ρ values. It was also confirmed from the tests' observations where the initial shear cracks extended parallel to the BFRP bars once they reached the bottom bars before extending diagonally in beams with high reinforcement ratios (R4 and R5), which enabled the beams to endure further shear strength before the concrete crushed. Similar phenomenon was also reported in Zarrinpour and Chao [32].

The plots shown in Fig. 10 (a) and (b) also indicated that using higher V_f of BMF enhanced the shear strength of all beams with different reinforcement ratios. For instance, at ρ of R1, the shear capacity of beams A-R1-0.75 (with V_f of 0.75%) and A-R1-1.5 (with V_f of 1.5%) was enhanced by 28 and 58%, respectively, over beam A-R1-0 cast with plain concrete. As previously stated, the bridging mechanism of the BMF across the diagonal cracks reduced the rate of crack widening, thus improving the shear resistance of concrete. This phenomenon was encountered in all beams of group A. A similar trend was obtained in beams of group B as illustrated in Fig. 10 (b). As an example, for beams with ρ of R1, the gain in shear capacity was 48 and 86% in beams B-R1-0.75 (with V_f of 0.75%) and B-R1-1.5 (with V_f of 1.5%), respectively, over beam B-R1-0 cast with plain concrete, indicating the significant effect of the added fibers on the shear strength even in beams with small a/d ratios.

Fig. 11 (a) and (b) shows the variation in the shear capacity of beams having different a/d ratios with the V_f of the added fibers. As shown in Fig. 11 (a), beams of group B (with ρ of R1) showed a more pronounced enhancement in their shear capacity with the addition of BMF than their

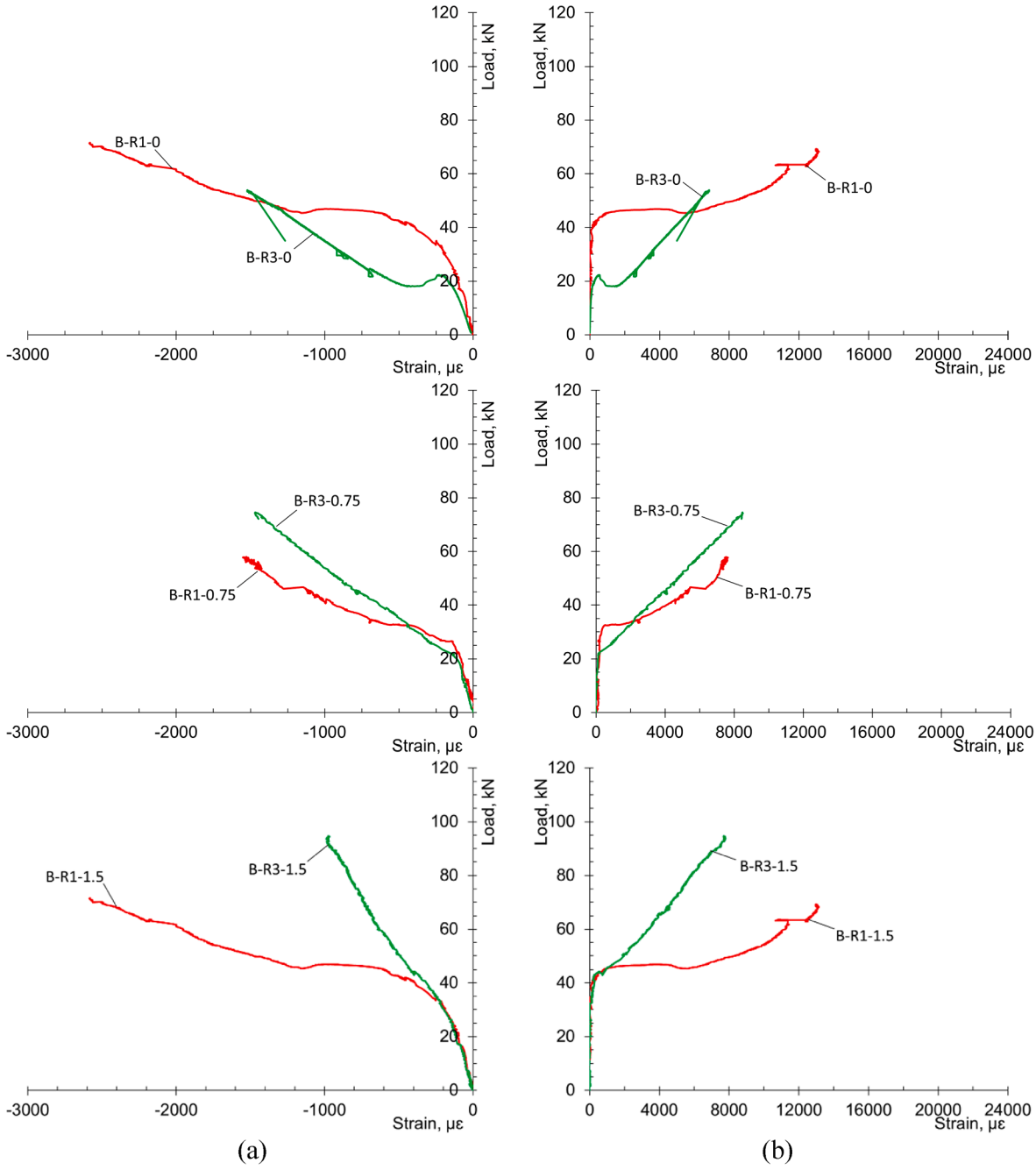

Fig. 9. Load-strain response of beams of group B: (a) strains in concrete and (b) strains in the BFRP bars.

counterparts of group A. For instance, beam B-R1-1.5 encountered 85% increase in its shear capacity versus 51% in beam A-R1-1.5. As depicted from Fig. 11 (b), increasing ρ to R3 offsets the BMF's impact on the shear strength of the beams. While beam B-R3-1.5 encountered an increase of 77% in its shear capacity due to the presence of 1.5% of BMF, beam A-R3-1.5 encountered an enhancement of 145% in its shear strength with the same volume of V_f provided. This finding was attributed to the fact that the shear caapcity of beams with small a/d ratios were mainly controlled by the arch action rather than the V_f of the added fibers.

4. Predicting the shear capacity of the tested beams

To estimate the shear capacity of the tested beams, three models were used, namely; the models developed by Gandomi et al. [33], Dinh et al. [34], and Arslan [35]. The formulations of each model are summarized in Table 5. It can be observed that each model incorporates several parameters that are known to contribute differently to the shear capacity of RC beams. Those parameters include the a/d ratio, the reinforcement ratio, ρ, the fiber bond factor, d_f, the fiber pull-out strength, ν_b, the volume fraction of the added fibers, V_f, the concrete compressive strength, f'_c, the fiber factor, F, and the interfacial bond stress factor, τ. It is important to note that the three models were originally designed to determine the shear strength of steel-reinforced concrete beams cast with steel-fiber-reinforced concrete mixes (SFRC). The model of Gandomi et al. [33] was developed using linear genetic programming on a database of 213 SFRC-cast beams reinforced with steel bars. Dinh et al. [34] assumed that the shear strength of SFRC-cast beams consisted of the vertical component of the diagonal tension of the steel fibers (across the diagonal shear crack) and the shear stress carried in the compression concrete zone. On the other hand, Arslan

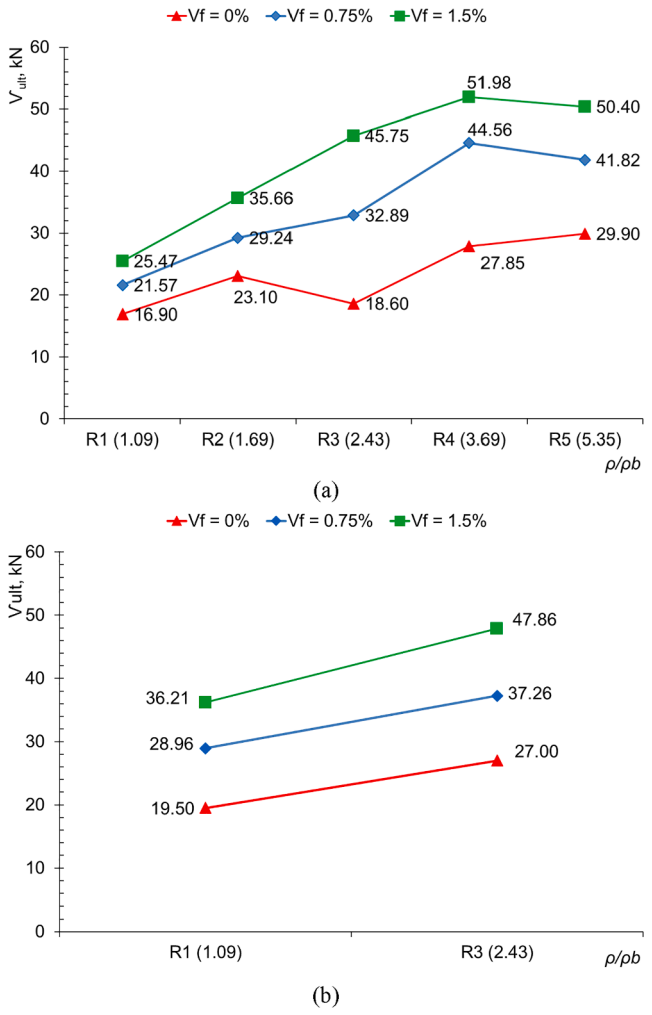

Fig. 10. Effect of the longitudinal reinforcement ratios on the shear capacity of beams of (a) group A and (b) group B.

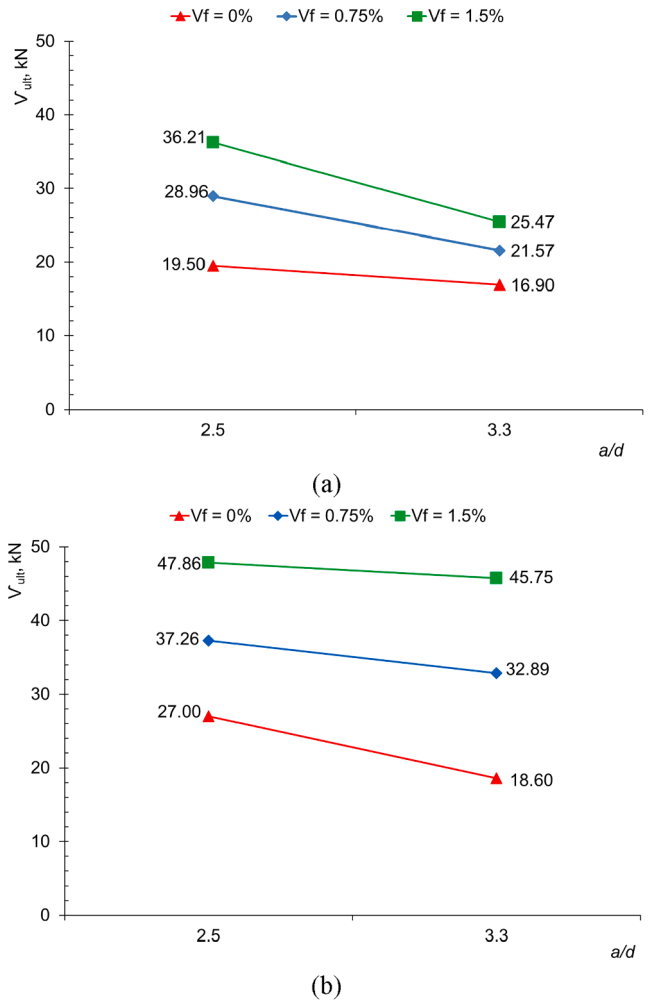

Fig. 11. Effect of span-to-depth ratios, a/d, on the shear capacity of beams with reinforcement ratio of (a) R1 and (b) R3.

[35] developed their model using basic mechanics principles while considering the slenderness ratio of the beam. Therefore, validating the ability of those models to estimate the shear capacity of the BFRC-BFRP beams of the current study is considered essential.

Table 6 compares the experimental and predicted shear capacity of beams of groups A and B. It can be observed that the shear capacity of all beams were overestimated by the models. The models of Gandomi et al. [33] and Dinh et al. [34] noticeably overestimated the shear capacity with average predicted-to-experimental capacity ratios, V_{pre}/V_{exp}, of 2.46 ± 0.64 and 2.01 ± 0.22, respectively, for beams of group A, and V_{pre}/V_{exp} of 2.48 ± 0.29 and 1.67 ± 0.11 for beams of group B, respectively. On the other hand, the shear capacity predicted by Arslan's model [35] was the closest to the experimental capacity with V_{pre}/V_{exp} ratios of 1.23 ± 0.13 and 1.15 ± 0.03 for beams of groups A and B, respectively. While Gandomi et al. [33], Dinh et al. [34], and Arslan [35] considered v_b, F, a/d, ρ, and $f_c^{'}$ in their models, they neglected the influence of the type of the longitudinal bars and the added fibers on the shear capacity of the beams, which clarified the overestimated predictions of the shear caapcity of all the tested beams.

4.1. Proposed model for shear capacity of BFRC–BFRP beams

The proposed model considered the type and amount of both the longitudinal reinforcement and the added fibers. The model is an adaption of two distinct models: the first model was utilized to calculate the concrete contribution to the shear strength of the BFRC-BFRP beams while the second model was used to calculate the contribution of the basalt fibers.

Table 5
Models predicting the shear strength of FRC-beams reinforced with longitudinal steel bars.

Model	Shear strength equations	Equation No
Gandomi et al. [32]	$v_u = \frac{2d}{a}(\rho f^{'}_c + v_b) + \frac{d}{2a}\frac{\rho}{(288\rho - 11)^4} + 2$	(1)
	$v_b = 0.41\tau F$	(2)
	$F = \left(\frac{L_f}{D_f}\right)V_f d_f$	(3)
Dinh et al. [33]	$v_u = 0.13\rho f_{fu} + 1.2\left(\frac{V_f}{0.0075}\right)^{\frac{1}{4}}\left(1 - \frac{c}{d}\right)$	(4)
	$c = 0.1h$	(5)
Arslan [34]	$v_u = \left(0.2 f^{'}_c{}^{\frac{2}{3}}\left(\frac{c}{d}\right)\left(1 + 0.032 f^{'}_c{}^{\frac{1}{6}}\right) + \sqrt{\rho(1 + 4F) f^{'}_c}\right)\left(\frac{3}{a/d}\right)^{\frac{1}{3}}$	(6)

In order to determine the concrete contribution to the shear strength of the BFRC-BFRP beams, the simplified empirical model of Ashour and Kara [36] presented in Eq. (7) was adopted. Ashour and Kara [36] developed this model based on a set of experimental data that consisted of 134 beams reinforced with different longitudinal FRP bars without stirrups using the design-by-testing approach. In their study, Ashour and

Table 6
Predicted-to-experimental ratios of the shear capacity of the BFRC–BFRP beams.

Beam		Gandomi et al. [32]		Dinh et al. [33]		Arslan [34]		Proposed Model	
	V_{exp}, kN	V_{pre}, kN	V_{pre}/V_{exp}	V_{pre}, kN	V_{pre}/V_{exp}	V_{pre}, kN	V_{pre}/V_{exp}	V_{pre}, kN	V_{pre}/V_{exp}
Group A (a/d = 3.3)									
A-R1-0.75	21.6	79.0	3.66	50.3	2.33	31.0	1.44	23.0	1.07
A-R1-1.5	25.5	87.9	3.45	57.0	2.24	37.3	1.47	30.4	1.19
A-R2-0.75	29.3	80.5	2.75	58.2	1.99	35.5	1.21	27.0	0.92
A-R2-1.5	34.5	89.5	2.60	64.8	1.88	43.1	1.25	36.1	1.05
A-R3-0.75	32.9	82.5	2.51	67.8	2.06	40.1	1.22	30.9	0.94
A-R3-1.5	40.5	91.7	2.27	74.5	1.84	49.0	1.21	41.6	1.03
A-R4-0.75	43.5	79.1	1.82	77.1	1.77	43.7	1.01	33.1	0.76
A-R4-1.5	50.8	87.9	1.73	83.1	1.64	53.6	1.06	45.2	0.89
A-R5-0.75	41.5	83.0	2.00	96.4	2.32	49.6	1.20	37.8	0.91
A-R5-1.5	50.4	92.1	1.83	102.3	2.03	61.2	1.22	52.0	1.03
Mean			2.46		2.01		1.23		0.98
SD			0.64		0.22		0.13		0.11
COV %			26.1		11.1		11.0		11.6
Group B (a/d = 2.5)									
B-R1-0.75	28.9	82.7	2.86	50.3	1.74	33.9	1.17	24.6	0.85
B-R1-1.5	36.2	94.3	2.61	57.0	1.58	40.8	1.13	32.0	0.88
B-R3-0.75	37.25	87.5	2.35	67.8	1.82	43.8	1.18	32.9	0.88
B-R3-1.5	47.8	99.5	2.08	74.5	1.56	53.6	1.12	43.7	0.92
Mean			2.48		1.67		1.15		0.88
SD			0.29		0.11		0.03		0.02
COV %			11.7		6.63		2.24		2.51

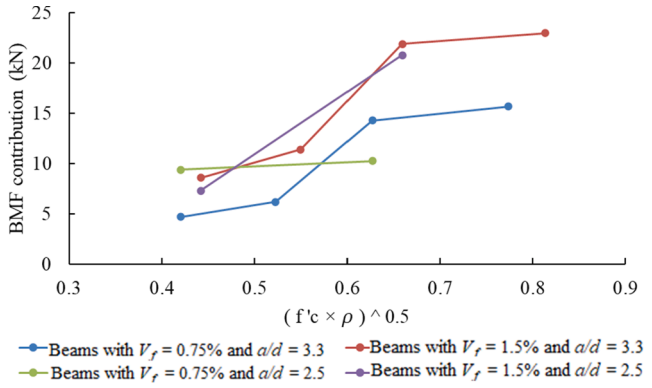

Fig. 12. The effect of $\sqrt{\rho f_c^{'}}$ on the shear contribution of BMF.

Kara [36] compared the results obtained from their model against several shear design methods such as JSCE-1997 [37], ACI 440.1R-06 [38], ISIS M03-07[39], CNR-DT 203/2006 [40], CSA-S806-02 [41] and reported the most accurate results for Eq. (7) with $V_{exp}/V_{pre} = 1.00 \pm 0.25$.

$$v_c = 2.2\left(\rho\frac{E_f}{E_s}\frac{d}{d}f_c^{'}\right)^{\frac{1}{3}} d \le 300mm \tag{7}$$

where E_f is the modulus of elasticity of the FRP longitudinal bars and E_s is that of the steel bars.

On the other hand, it has been well established in the literature that the fiber contribution to the shear capacity depends on several factors such as L_f/D_f, d_f, V_f, and $f_c^{'}$ [42–46]. Thus, the same variables were considered to develop a model that accounted for the impact of BMF on the shear strengths of the tested beams. To do so, the shear strengths of the tested beams were first compared to those reported in El Refai and Abed [10]. In their study, El Refai and Abed [10] tested 8 plain concrete beams reinforced with BFRP bars. As previously mentioned, the beams had comparable sizes, a/d ratios, ρ, and mix proportions to the beams utilized in this study. Therefore, the difference between the shear strengths of the beams tested in the current study and those of their counterparts in El Refai and Abed [10] was considered as the contribution of the BMF to the shear strength, V_{BMF}, of the tested beams, as shown in Table 4.

Fig. 12 shows the relationship between V_{BMF} and the factor $\sqrt{\rho f_c^{'}}$ for all the tested beams. It can be noticed that the contribution of BMF to the shear strengths was more pronounced when $\sqrt{\rho f_c^{'}}$ increased, which can be attributed to the enhanced dowel action and the bonding characteristics that retards the slippage of the bars and the crack widening. Hence, a regression analysis was conducted on the V_{BMF} results calculated in Table 4 and Eq. (8) was then suggested to predict the BMF's impact on the shear strength of the beams while taking into account the factors ρ, $f_c^{'}$, $\left(\frac{L_f}{D_f}\right)$, V_f, and d_f as follows:

$$v_f = 1.79\left(\frac{L_f}{D_f}\right)V_f d_f\sqrt{\rho f_c^{'}} \tag{8}$$

Thus, the shear capacity of the tested beams was predicted by merging Eq. (7) and (8) in Eq. (9) as follows:.

$$v_{BFRC-BFRP} = 2.2\left(\rho\frac{E_f}{E_s}\frac{d}{d}f_c^{'}\right)^{\frac{1}{3}} + 1.79\left(\frac{L_f}{D_f}\right)V_f d_f\sqrt{\rho f_c^{'}} \tag{9}$$

Eq. (9) clearly shows that the proposed model takes into account all variables that are deemed affecting the shear strength of the BFRC-BFRP beams, including the dowel effect of the BFRP bars, the a/d ratio, the $f_c^{'}$, and the BMF effect.

4.2. Validation of the proposed model

The experimental capacity of the BFRC-BFRP beams were compared to the predicted capacity obtained by the proposed model and that obtained by the models of Gandomi et al. [33], Dinh et al. [34], and Arslan [35]. The predicted-to-experimental ratios, V_{pre}/V_{exp}, obtained are summarized in Table 6 and compared in Fig. 13. It can be noticed that the proposed model produced the most accurate predictions of the shear capacity with average V_{pre}/V_{exp} ratios of 0.98 ± 0.11 and 0.88 ± 0.02 for beams of groups A and B, respectively.

5. Conclusions and recommendations

In this study, the shear performance of concrete beams reinforced

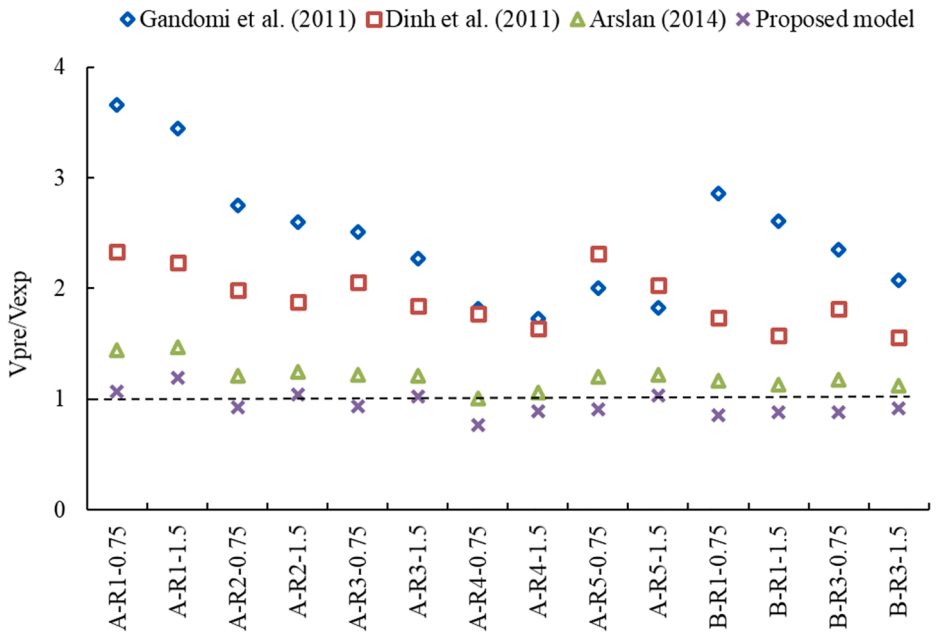

Fig. 13. Comparison between the predicted-to-experimental shear capacities, V_{pre}/V_{exp}, of the BFRC-BFRP beams.

longitudinally with BFRP bars and cast with BFRC mixes incorporating basalt macro-fibers (BMF) was investigated. The experimental shear capacity of the tested beams were predicted using the formulations of existing models, which were developed to predict the shear capacity of steel-reinforced beams cast with SFRC mixes. A model that considered the type and amount of both the longitudinal reinforcement and the added fibers was proposed. The following conclusions can be drawn from the study:.

- All the tested beams failed in shear showing one main diagonal crack. Beams cast with BFRC mixes developed more flexural cracks at failure compared to those cast with plain concrete.
- The BMF delayed the formation of the shear cracks and limited their widening owing to the bridging effect of the fibers between the cracked surfaces. All beams cast with BFRC mixes had flatter diagonal cracks at failure than their control beams indicating that the addition of BMF to the concrete mixes improved the shear resistance of concrete.
- Beams of group A with $a/d = 3.3$ experienced an increase in their shear strengths of 46 and 81% for V_f of 0.75 and 1.5%, respectively, compared to their control beams whereas beams of group B with $a/d = 2.5$ had an average increase in their shear strengths of 43 and 82% for the same volume fractions, respectively.
- The shear performance of beams of group B was governed by the arch action rather than the volume fraction, V_f, of the BMF. As a result, the impact of the longitudinal reinforcement ratio,ρ, on the shear strength of those beams was more pronounced than that of V_f.
- All the existing models used in the analysis overestimated the shear strengths of the BFRC-BFRP beams. However,the model of Arslan [35] predicted the shear strengths of the tested beams with the closest average predicted-to-experimental ratios, V_{pre}/V_{exp}, of 1.23 $\pm$ 0.13 and 1.15 $\pm$ 0.03 for beams with a/d ratios of 3.3 and 2.5, respectively.
- The proposed model incorporated the type and amount of the longitudinal reinforcing bars and the discrete fibers. The model demonstrated acceptable shear strength predictions of the tested BFRC-BFRP beams with average ratios V_{pre}/V_{exp} of 0.98 $\pm$ 0.11 and 0.88 $\pm$ 0.02 for beams with a/d ratios of 3.3 and 2.5, respectively.

Finally, this study has confirmed the promising use of basalt macro-fibers (BMF) to enhance the shear capacity of hybrid BFRC-BFRP beams. More experimental data are still needed to investigate the effect of other parameters on the shear performance of RC beams and to validate the proposed model when different types of FRP bars and composite fibers are used. Future investigations should also tackle the durability and long-term performance of the BMF utilized in this study under various environmental conditions.

CRediT authorship contribution statement

Ahmed El Refai: Conceptualization, Methodology, Validation, Writing – review & editing, Supervision. **Wael Alnahhal:** Conceptualization, Methodology, Validation, Writing – review & editing, Resources, Funding acquisition, Supervision, Project administration. **Abathar Al-Hamrani:** Investigation, Formal analysis, Writing – review & editing, Data curation, Software. **Sarah Hamed:** Investigation, Formal analysis, Visualization.

Declaration of Competing Interest

The authors declare that they have no known competing financial interests or personal relationships that could have appeared to influence the work reported in this paper.

Acknowledgment

The authors would like to express their appreciation to the Qatar Foundation for their financial assistance through UREP award no. UREP21-089-2-039 and GSRA grant no. GSRA6-1-0301-19005 from the Qatar National Research Fund (QNRF, a member of Qatar Foundation).

Data Availability

The raw/processed data required to reproduce these findings cannot be shared at this time as the data also forms part of an ongoing study.

References

[1] Alkhrdaji. T, Wideman. M, Belarbi. A NA. Shear strength of GFRP RC beams and slabs. In: Figueiras J, Juvandes L, Furia R, Porto P, editor. Proc, 2nd Int Conf Compos Constr; 2001. p. 409–414.

[2] Yost JR, Gross SP, Dinehart DW. Shear strength of normal strength concrete beams reinforced with deformed GFRP Bars. J Compos Constr 2001;5(4):268–75.
[3] Tureyen AK, Frosch RJ. Shear tests of FRP-reinforced concrete beams without stirrups. ACI Struct J 2002;99:427–34. https://doi.org/10.14359/12111.
[4] Al-Hamrani A, Alnahhal W. Shear behavior of basalt FRC beams reinforced with basalt FRP bars and glass FRP stirrups: Experimental and analytical investigations. Eng Struct 2021;242:112612. https://doi.org/10.1016/j.engstruct.2021.112612.
[5] Al-Hamrani A, Alnahhal W, Elahtem A. Shear behavior of green concrete beams reinforced with basalt FRP Bars and Stirrups. Compos Struct 2021;277:114619. https://doi.org/10.1016/j.compstruct.2021.114619.
[6] American Concrete Institute (ACI) Committee 440. Guide for the Design and Construction of Structural Concrete Reinforced with Fibre-Reinforced Polymer (FRP) Bars (ACI 440.1R-15). 2015. Doi: 10.1061/40753(171)158.
[7] CSA (Canadian Standards Association). Canadian highway bridge design code. CAN/CSA-S6-14, Mississauga, ON, Canada.: 2014.
[8] CSA (Canadian Standards Association). Design and construction of building components with fiber reinforced polymers. (CSA-S806-12) 2012.
[9] Issa MA, Ovitigala T, Ibrahim M. Shear Behavior of Basalt Fiber Reinforced Concrete Beams with and without Basalt FRP Stirrups. J Compos Constr 2016;20 (4):04015083. https://doi.org/10.1061/(ASCE)CC.1943-5614.0000638.
[10] El Refai A, Abed F. Concrete Contribution to Shear Strength of Beams Reinforced with Basalt Fiber-Reinforced Bars. J Compos Constr 2016;20(4):04015082. https://doi.org/10.1061/(ASCE)CC.1943-5614.0000648.
[11] Mahmoud K, El-Salakawy E. Shear strength of GFRP-reinforced concrete continuous beams with minimum transverse reinforcement. J Compos Constr 2014; 18:1–11. https://doi.org/10.1061/(ASCE)CC.1943-5614.0000406.
[12] Awadallah ZH, Ahmed MM. Journal of Engineering Sciences Faculty of Engineering some parametrs affecting shear behavior of high strength fiber reinforced concrete beams. J Eng Sci 2014;42:1163–78.
[13] Said M, Adam MA, Mahmoud AA, Shanour AS. Experimental and analytical shear evaluation of concrete beams reinforced with glass fiber reinforced polymers bars. Constr Build Mater 2016;102:574–91. https://doi.org/10.1016/j.conbuildmat.2015.10.185.
[14] Attia K, Alnahhal W, Elrefai A, Rihan Y. Flexural behavior of basalt fi ber-reinforced concrete slab strips reinforced with BFRP and GFRP bars. Compos Struct 2019;211:1–12. https://doi.org/10.1016/j.compstruct.2018.12.016.
[15] Abushanab A, Alnahhal W. Numerical parametric investigation on the moment redistribution of basalt FRC continuous beams with basalt FRP bars. Compos Struct 2021;277:114618. https://doi.org/10.1016/j.compstruct.2021.114618.
[16] Abushanab A, Alnahhal W, Farraj M. Structural performance and moment redistribution of basalt FRC continuous beams reinforced with basalt FRP bars. Eng Struct 2021;240:112390. https://doi.org/10.1016/j.engstruct.2021.112390.
[17] Taha A, Alnahhal W, Alnuaimi N. Bond durability of basalt FRP bars to fiber reinforced concrete in a saline environment. Compos Struct 2020;243:112277. https://doi.org/10.1016/j.compstruct.2020.112277.
[18] Li VC, Ward R, M.Hamza A. Steel and synthetic fibers as shear reinforcement. ACI Mater J 1992;89:499–508.
[21] Ding Y, You Z, Jalali S. The composite effect of steel fibres and stirrups on the shear behaviour of beams using self-consolidating concrete. Eng Struct 2011;33(1): 107–17. https://doi.org/10.1016/j.engstruct.2010.09.023.
[22] Minelli F, Plizzari G. Steel fibers as shear reinforcement for beams. Proc. Second fib Congr., Naples, Italy: 2006.
[23] Gopinath S, Meenu S, Ramachandra MA. Shear strength evaluation of concrete beams reinforced with BFRP bars and steel fibers without stirrups. Comput Mater Contin 2016;51:81–103. https://doi.org/10.3970/cmc.2016.051.081.pdf.
[24] Adhikari S. Mechanical and Structural Characterization of Mini-Bar Reinforced Concrete Beams. The University of Akron; 2013.
[25] Fan X, Xu T, Zhou Z, Zhou X. Experimental Study on Basic Mechanical Properties of BFRP Bars. IOP Conf Ser: Mater Sci Eng 2017;250:012014. https://doi.org/10.1088/1757-899X/250/1/012014.
[26] Vajje S, Krishna NR. Study On Addition Of The Natural Fibers Into Concrete. Int J Sci Technol Res 2013;2:213–8.
[27] Kizilkanat AB, Kabay N, Akyüncü V, Chowdhury S, Akça AH. Mechanical properties and fracture behavior of basalt and glass fiber reinforced concrete: An experimental study. Constr Build Mater 2015;100:218–24. https://doi.org/10.1016/j.conbuildmat.2015.10.006.
[28] Branston J, Das S, Kenno SY, Taylor C. Mechanical behaviour of basalt fibre reinforced concrete. Constr Build Mater 2016;124:878–86. https://doi.org/10.1016/j.conbuildmat.2016.08.009.
[29] ASTM C469/C469M-14. Standard Test Method for Static Modulus of Elasticity and Poisson ' s Ratio of Concrete. West Conshohocken: 2014. Doi: 10.1520/C0469.
[30] Attia K, El Refai A, Alnahhal W. Flexural Behavior of Basalt Fiber-Reinforced Concrete Slab Strips with BFRP Bars: Experimental Testing and Numerical Simulation. J Compos Constr 2020;24(2):04020007. https://doi.org/10.1061/(ASCE)CC.1943-5614.0001002.
[31] Sahoo DR, Maran K, Kumar A. Effect of steel and synthetic fibers on shear strength of RC beams without shear stirrups. Constr Build Mater 2015;83:150–8. https://doi.org/10.1016/j.conbuildmat.2015.03.010.
[32] Zarrinpour MR, Chao SH. Shear strength enhancement mechanisms of steel fiber-reinforced concrete slender beams. ACI Struct J 2017;114:729–42. https://doi.org/10.14359/51689449.
[33] Gandomi AH, Alavi AH, Yun GJ. Nonlinear modeling of shear strength of SFRC beams using linear genetic programming. Struct Eng Mech 2011;38(1):1–25. https://doi.org/10.12989/sem.2011.38.1.001.
[34] Dinh HH, Parra-Montesinos GJ, Wight JK. Shear Strength Model for Steel Fiber Reinforced Concrete Beams without Stirrup Reinforcement. J Struct Eng 2011;137 (10):1039–51. https://doi.org/10.1061/(ASCE)ST.1943-541X.0000362.
[35] Arslan G. Shear Strength of Steel Fiber Reinforced Concrete (SFRC) Slender Beams. J Civ Eng 2014;18(2):587–94. https://doi.org/10.1007/s12205-014-0320-x.
[36] Ashour AF, Kara IF. Composites: Part B Size effect on shear strength of FRP reinforced concrete beams. Compos PART B 2014;60:612–20. https://doi.org/10.1016/j.compositesb.2013.12.002.
[37] JSCE(Japan Society of Civil Engineers). Recommendation for design and construction of concrete structures using continuous fiber reinforcing materials. 1997:1–58.
[38] American Concrete Institute (ACI) Committee 440. "'Guide for the design and construction of structural concrete reinforced with FRP bars"'. Farmington Hills, MI, USA: ACI 440.1R-06, American Concrete Institute; 2006.
[39] ISIS M03-07. Reinforcing concrete structures with fiber reinforced polymers. ISIS-M03-07, Canadian network of centers of excellence on intelligent sensing for innovative structures, Univ. of Winnipeg, Winnipeg, Man; 2007.
[40] CNR-DT-203/2006. Guide for the design and construction of concrete structures reinforced with fiber-reinforced polymer bars. National Research Council, Rome, Italy; 2007:39.
[41] CSA (Canadian Standards Association). Design and construction of building components with fibre-reinforced polymers. Canadian Standards S806-02, 2002. Ontario, Canada: Rexdale. (CSA-S806-02) 2002.
[42] Narayanan R, Darwish IYS. Use of Steel Fibers as Shear Reinforcement. ACI Struct J 1987;84:216–27. https://doi.org/10.14359/2654.
[43] Al-Ta'an SA, Al-Feel JR. Evaluation of shear strength of fibre-reinforced concrete beams. Cem Concr Compos 1990;12(2):87–94. https://doi.org/10.1016/0958-9465(90)90045-Y.
[44] Swamy RN, Jones RCA. Influence of steel fibres on the shear resistance of lightweight concrete T-beams. ACI Struct J 1993;90:103–14.
[45] Khuntia M, Stojadinovic B, Goel SC. Shear strenght of normal and high-streng fiber reinforced concrete beams without stirrups. ACI Struct J 1999;99:530–8.
[46] Singh B, Jain K. Appraisal of steel fibers as minimum shear reinforcement in concrete beams. ACI Struct J 2014. https://doi.org/10.14359/51686969.